



Review of manufacturing three-dimensional-printed membranes for water treatment

Merlin N. Issac¹ · Balasubramanian Kandasubramanian²

Received: 27 January 2020 / Accepted: 26 May 2020 / Published online: 6 July 2020
© Springer-Verlag GmbH Germany, part of Springer Nature 2020

Abstract

With the exacerbation of industrialization, water treatment has become a necessary step for the eradication of dyes, heavy metals, oils, pharmaceuticals, and illicit drugs. These pollutants pose an impending threat to the health of humans by causing chronic or acute poisoning. Albeit they are noxious, the presence of some metals in lower concentrations is indispensable for human health. 3D printing (additive manufacturing) (3DP) can contrive nearly any complicated geometric form in a wide array of objects among various scales by a layer-wise method of manufacturing, which is more indubitably designed than any other conventional method. 3DP could remodel the existing patterns of membrane housing and possibly trim down the power demand and chemical use in saltwater desalinating and wastewater purification plants. Membranes that are 3D printed with correctly arranged apertures and shapes enhance material transport and flow athwart the surface of the membrane and at once lessen membrane soiling. This kind of technology forges membranes of polymers, biopolymers, alloys, metals, and ceramics via computer-aided design (CAD). A polylactic acid porous super-hydrophobic membrane with pore size in the range 40–600 μm showed 99.4% oil-water separating power and 60 $\text{kL h}^{-1} \text{m}^{-2}$ flux when the pore size was tuned to 250 μm via CAD-aided 3D printing technology. This review focuses on the ability of 3D-printed membranes for the efficient removal of toxic pollutants from wastewater.

Keywords Toxic pollutants, 3D printing, Additive manufacturing, 3D printed membranes, Polylactic acid, Separation efficiency

Introduction

Burgeoning industrialization and change in lifestyles had vandalized water reservoirs with malevolent pollutants from industries, households, and agriculture (use of pesticides and fertilizers) that may enter the food web, causing acute diseases. Intake of the unendurable amount of such pollutants as a result of water absorption may upshoot their inrush in blood circulation and results in severe medical conditions (Singh et al. 2011). As the world's population continues to grow, accessible water supplies will become increasingly

exiguous. Wastewaters have a broad spectrum of concentrations and coalescence of pollutants that pose a thumping menace to life due to bioaccumulation and biomagnifications; thence, watercourses should be dealt as economical as feasible and in an unassailable mode by processes that are user friendly and that demands minimal labor. Bio-magnification (Kelly et al. 2007) is the process by which toxic pollutants are conceded on from one tropic level to the other within a food web, resulting in chronic diseases affecting the brain, skin, and cardiovascular, hepatic, renal, and respiratory systems. Water-treatment confiscates contaminants and undesirable components or truncates their absorption so that the water becomes fit for its desired use. Membranes served as the prime device for removing substances from water and may also apply in concurrence with other physicochemical procedures to part or to make two phases in contact among themselves (Gonte and Balasubramanian 2012; Gonte et al. 2013; Arora et al. 2014; Verma and Balasubramanian 2014; Bhalara et al. 2014; Gore et al. 2016a, b; 2018a, b; 2019a, b, c; Khanale and Balasubramanian 2016; Sharma et al. 2016; Davis and Balasubramanian 2016; Gupta and Kandasubramanian 2017; Gore and Kandasubramanian 2018; Saini and

Responsible editor: Angeles Blanco

✉ Balasubramanian Kandasubramanian
meetkbs@gmail.com

¹ CIPET: Institute of Plastics Technology (IPT), HIL Colony, Edayar Road, Pathalam, Eloor, Udyogamandal P.O, Kochi, Kerala 683501, India

² Department of Metallurgical and Materials Engineering, Defence Institute of Advanced Technology (DU), Girinagar, Pune, Maharashtra 411025, India

Kandasubramanian 2018; Kalathil et al. 2019; Rajhans et al. 2019). Three-dimensional (3D)-printed membranes are used in water treatment because it improves some of the disadvantages of membranes like lack of reliability, slow operation, reduced selectivity, and elevated cost along with some additional properties like easy control of membrane fouling, low-energy consumption, and abrasion resistance. Materials used for 3D printing (3DP) include metals, polymers like polyamide, polylactic acid, ceramics, and alloys (Mazumder and Cole 2003; Hyde et al. 2014). 3DP offers the prospective to corroborate the generative manufacturing of these materials when compared with conventional manufacturing used in purification technologies of water (Berman 2012). 3DP or rapid prototyping is a layer-wise fashioning of objects that compile parts from 3D model data, rather than reductive manufacturing and is also known as additive manufacturing (AM) (Shirazi et al. 2015; Yap et al. 2015). 3DP uses a process involving four steps that begin with designing the model using computer-aided design (CAD), then transformation into readable STL format, and eventually carving the model into numerous 2D layers before 3D printer modeling (Chua et al. 2017). Compared with traditional manufacturing techniques such as mechanization, molding, and trampling that contrive outputs by effacing objects from a more massive stock, AM forges the definite form by appending objects, thereby making effective utilization of raw materials and generate marginal waste attaining a middling geometrical accuracy (Kruth et al. 1998; Levy et al. 2003). Besides water treatment, other applications unfurl to usage in different sectors like aeronautics, biomedical, construction, etc. (Lee et al. 2016b; Gupta et al. 2016; Yadav et al. 2017, 2018; Korde et al. 2018; Mishra and Kandasubramanian 2018; Deoray and Kandasubramanian 2018; Malik and Kandasubramanian 2018; Gharde et al. 2019a, b; Korde and Balasubramanian 2019; Rastogi and Kandasubramanian 2019a, b; Prasad and Kandasubramanian 2019; Rastogi et al. 2019; Gautam et al. 2020). 3DP, involving different methodologies and materials, flourished over recent years with the propensity to convert manufacturing processes. Utilization of 3DP depreciated the extra expenditures during the litigation of material development. The growing recognition of the 3D system in comparison with conventional methods has multiple benefits, comprising modeling of intricate geometrical shapes with high accuracy, maximized material frugality, design flexibility, customization (Ivanova et al. 2013), and excessive adjustability for various materials. Additive manufacturing is used for manufacturing separation membranes with different forms, dimensions, and porosities, which could not be consummated by using traditional mechanical processes like electrospinning and tape casting (Dommati et al. 2019). The resolution limits for fabricating membrane ranges from 0.1 to 10 μm , which accentuates a diminution in the applicability of 3DP to print large-sized porous membranes (Lee et al. 2016b). The membrane flux

(Xing et al. 2018) is determined by computing the volume of permeate per area of membrane per unit time by Eq. (1).

$$\text{Flux} = \frac{V}{St} \quad (1)$$

where V is the volume of permeate, S is the active area of the membrane, and t is the period of operation. Percentage of adsorption (Gonte et al. 2014) is determined by Eq. (2) where C_o is the initial concentration and C_e is the final concentration.

$$\% \text{adsorption} = \frac{(C_o - C_e)}{C_o} \times 100 \quad (2)$$

Membrane modeling via additive manufacturing can be distinguished based on raw materials and methods used for layer-wise structure design (Zhakeyev et al. 2017). 3D techniques for membrane fabrication include material jetting, powder bed fusion (Mousavi et al. 2018), binder jetting (Chua et al. 1998), material extrusion (Alaimo et al. 2017), vat photo-polymerization (Bui et al. 2015), sheet lamination (Gibson et al. 2015), and direct energy deposition. The critical components in membrane technology comprise membrane modules such as hollow fiber (HFM), spiral wound (SWM), and plate and frame (PFM). Ascribable to their complicated behavior and manufacturing limits, their performance is challenging to optimize. By length scale, components of membrane modules are classified into membranes, spacers, and modules. In terms of pore size, flat sheet, or hollow fiber membrane (Giwa et al. 2016), they are in sub-nanometer to micrometer scale, with flow channel spacers in the millimeter scale while module at the centimeter to meter scale (Lee et al. 2016b). In the membrane module, the function of the spacer is to augment the overall transfer of material to ease the concentration polarization effect. Conversely, the interaction between membrane and spacer could escort to the fouling of membrane due to spacer's "shadow effect," leading to fouling accretion on the membrane, and it can also be stimulated by the spacer alone (Vrouwenvelder et al. 2009). Optimization of spacers by the amalgamation of 3DP technology and membrane housing addresses the fouling problem by escalating massive transportation and plummeting concentration polarization at the plane of the membrane. 3DP could transfigure the membrane housing design and potentially trim down the energy consumption and usage of chemicals in wastewater treatment plants (Lee et al. 2016b). This review illustrates the capability of 3D-printed membranes for the efficient annihilation of noxious pollutants from wastewater. Membranes are approved because of their simple, unswerving, and low-cost manufacturability. A concise idea of the toxicity of pollutants, membrane filtration, AM, processing methods, and 3DP membranes is described in this review. Accordingly, the various 3DP membranes used in water treatment appraised from various articles and their future perspectives are provided. Due to impending

beneficial impacts for manufacture and adaptability with various materials, 3DP promises in the membrane technology fields. From this review, it can culminate from the membrane being defiant to breakage and fouling and have the potential to confiscate toxic pollutants efficiently.

Toxicity of water pollutants

Heavy metals are metallic natural elements that shall include mercury (Hg), cadmium (Cd), copper (Cu), arsenic (As), etc., having a higher density of about $3.5\text{--}7\text{ g cm}^{-3}$ that is pernicious at lower concentrations. As they are non-biodegradable, they get accrued in the biotic system, once ingested (Gautam et al. 2014).

Mercury present in various types comprises inorganic mercury that includes metallic mercury, mercury vapor (HgO), and mercurous (Hg⁺) or mercuric (Hg²⁺) salts; and organic mercury involves mercury-bonded carbon-containing compounds (Bernhoft 2012). Toxicity of mercury depends on forms, dosage, and exposure rate; mercuric vapor damages the brain, whereas mercury salts target the intestinal epithelium and kidney. The acute and enduring effects of mercuric salts, alkoxy alkyl mercury, and phenyl mercury compounds are liable for digestive disorders and kidney failure appearing as renal tubular acidosis, with acute tubular necrosis in grave cases. In humans, the fatal dosage of mercuric salt is about 1 g (Berlin et al. 2015). Methyl mercury that is widely distributed throughout the body is responsible for cytotoxicity, including lipid peroxidation, neurotoxic molecule accumulation, and microtubule damage (Patrick 2002). According to the WHO, the TDI of Hg²⁺ for safe drinking water is $6\text{ }\mu\text{g L}^{-1}$ allowing a 60-kg adult 2 L of water day⁻¹ (Rastogi and Kandasubramanian 2019c).

Arsenic, a carcinogen (Farrell et al. 2001), when taken in trifle quantity, is a vital alimentary element, but ancillary uptake at $> 10\text{ }\mu\text{g L}^{-1}$ may cause pernicious effects like malignancy and heart diseases; also, its soluble and insipid trait makes it further precarious (Gore et al. 2018a). Contamination of arsenic eventuate from both natural phenomena such as weathering of minerals comprising arsenic and anthropic actions like unbridled industrial effluents from mining and metal industries and use of organo-arsenical pesticides (Krishna et al. 2001) existing in different forms in which arsenate As(V) accounts for 60%, as sulfide 20% and the extant 20% for arsenites, arsenide, silicates, oxides, and elemental arsenic (Mandal 2002). The primary forms of arsenic are arsenate(V) and arsenite(III) (Ferguson and Gavis 1972) and are present in the environment as the oxoanions arsenate (AsO_4^{3-}) and arsenite (As(OH)_3), respectively, in which arsenite(III) has greater mobility in groundwater and is most poisonous than arsenate(V). Arsenite is thermodynamically stable under low pH and exists as arsenous acid. The order of toxicity of arsenicals is determined by the criterion

of seepage of intracellular potassium and lactic acid dehydrogenase (LDH), and the mitochondrial metabolism of the tetrazolium salt is monomethylarsonous acid(III) $>$ As(III) $>$ As(V) $>$ monomethylarsonous acid (V) = dimethylarsinic acid(V). The intermediary product monomethylarsonous acid(III) in arsenic biotransformation is noxious than any other arsenic compounds and is liable for oncogenesis and other effects (Singh et al. 2007).

Chromium, the seventh most ample element in nature (Oliveira 2012), has multiple oxidation states, but the most stable are + 2, + 3, and + 6. Cr(VI) is a strong epithelial irritant and is also a carcinogen present as CrO_4^{2-} and $\text{Cr}_2\text{O}_7^{2-}$ forms. Chromium trioxide is highly poisonous, as it provides a soaring solubility and motility athwart membranes in living organisms and the surroundings. Chromium(III), a micronutrient in humans obligatory for sugar and lipid metabolism presents as oxides, sulfates, and hydroxides, show lower toxicity as it turns out to be indissoluble in water, exhibiting lower motion and is bound to the organic compounds in aquatic and soil environments (Becquer et al. 2003). According to the WHO health guidelines, TDI of chromium is 0.05 mg L^{-1} (Rastogi and Kandasubramanian 2019c).

Oil, a mixture of different chemicals that vary with its proportions, is a contentious subject due to toxicity (Tatem et al. 1978). Pollution due to industrial expulsion and oil spill leakage not only affects health but also results in undesirable impacts on the environment. Momentous sources of oil include accidental oil spills from tankers, pipelines, and other offshore sites that store oils. Due to high cost, low efficiency, and high-energy consumption of conventional methods like physical adsorptions, dispersant treatment, in situ burning, and chemical coagulants, more cost-effective methods are taken to treat water using membrane technology (Xing et al. 2018).

Discharges from industries like paint, textile, etc. result in large quantities of dyes in waters that are water soluble and introduce adverse effects due to inherent noxiousness and daylight, impeding dye properties (Mousavi et al. 2018). Pharmaceuticals designed to be attuned with the biotic system also cause detrimental waste.

As the world population rises, there is a surge in food and energy demand, therefore water supplies are required for domestic and agricultural uses, so due to water shortage, numerous attempts were undertaken to treat wastewater and exclude hazardous metals before disposal since 80% of wastewater is released mostly to the atmosphere even without treatment or reuse. The largest trigger of natural water contamination is industrial-treated metal-contaminated wastewater; metal pollutants are stable and thus do not degrade in aquatic habitats. The most prevalent contaminants in water supplies are heavy metal ions that are noxious, even in small quantities, and can pose difficulties in human health and therefore needs to be dealt with, before discharging into the ecosystem. Common

ways of extracting heavy metal ions from aquatic environments include coagulation-flocculation, exchange of ions, electrochemical deposition, crystallization, and chemical precipitation. Many of these methods have major drawbacks, such as the sequence of heterogeneous reactions or the transfer of substances between various stages typically taking a long operation term and a high level of reagent, producing toxic waste that needs disposal. However, concerning the imminent water crisis, the research scientists have worked on developing environmentally sustainable membrane-based water treatment systems that use relatively limited quantities of energy. The main objective is to develop a membrane to improve the separation performance, especially to remove the toxic pollutants from aqueous solutions (Shukla et al. 2018, 2019).

Filtration using membranes

Water purification technologies employ various membrane forms that involve membranes of microfiltration, ultrafiltration, reverse osmosis, and nanofiltration. Microfiltration membranes have large-sized pores of about 0.03 to 10 μm that reject larger particles and other microorganisms. Microfiltration does not pose a total obstacle to the virus. Nevertheless, microfiltration helps to regulate certain microorganisms in the water when applied in conjunction with disinfection. Increasing attention is focused on curtailing the concentration and amount of chemicals used throughout water purification. Membrane filtration can substantially minimize the number of chemicals added, by the physical removal of pathogens.

Ultrafiltration membranes with pore size 0.002 to 0.1 μm smaller than microfiltration membrane have an operational pressure of around 200–700 kPa and resist bacteria and other soluble macro-molecules together with larger particles and microorganisms. The major benefits of ultrafiltration membranes are chemical-free nature and easy automation, but fouling may trigger water treatment problems in membrane technologies. Non-porous reverse osmosis membranes remove particles and also other low-molar species, including salt ions, organics, etc. Reverse osmosis eliminates almost all contaminants and performs instantly with little or no break-in time. Major drawbacks of reverse osmosis are a higher price, wastewater generation, requirement of pretreatments, and vulnerability to fouling. Nanofiltration membranes have pores in the order of ten or fewer angstroms thus exhibiting efficiency between the reverse osmosis and ultrafiltration membranes. The flow of water across the small pores of the membrane demands an operating pressure of 600–1000 kPa which is greater than both micro- and ultrafiltration. Nanofiltration membrane is often referred to as softening membranes as it reduces water hardness but may require pretreatment to prevent precipitations. Nevertheless, nanofiltration takes a lot of energy than microfiltration or ultrafiltration (Amjad 1993).

Most membranes of the microfiltration, ultrafiltration, reverse osmosis, and nanofiltration are organic synthetic polymers. Micro- and ultrafiltration membranes are mostly manufactured from similar materials yet are designed under varying membrane-forming conditions to create distinct-sized pores. The membrane can be made also from ceramics or metals. Microporous ceramic membrane shows thermal stability, resistance to chemicals, and is mostly used for microfiltration. But, their widespread usage has been hampered by drawbacks such as heavy costs and mechanical frailty. Finely pored metallic membranes are primarily used in gas separations, but they can even be utilized in higher-temperature water treatment applications or as a support for membranes. Over the past few decades, comprehensive studies have thoroughly investigated the manufacture of membranes for specific applications in desalinization and water purification by various methods including phase inversion, interfacial polymerization, track etching, and electrospinning to generate high-performing membranes in terms of selectiveness and conductance. The use of high quantities of solvents that can be hazardous and the resulting pollution causing waste, the lower porosity and permeability of the membranes thus produced, and the cost impedes the widespread implementation of traditional methods.

The membrane technology continues to advance with the demonstrated performance of the membranes in the water purification field. Key issues that still need focus are membrane soiling and chemical stability of the membrane. Consequently, diminished soiling will potentially make membranes much more price effective by expanding their operating life and reducing their demands for energy.

However, with the advent of 3D printing, a system of membrane manufacturing with complete regulation of membrane structure was carried out at low cost and without the extensive use of solvents. The potential of three-dimensional printing to produce complex structures and sizes with precision promises for membrane manufacturing (Tijing et al. 2020). Table 1 discusses about various membrane fabrication techniques along with their benefits and drawbacks.

3D printing

Additive manufacturing or 3DP technology fabricates a part through CAD software that forges objects from the bottom to the upper region by appending materials into layers cross-sectionally one at a time. The computer designs translate into physical models in 3D printing through the layered patterning of material extruded via print head, nozzle, or other mechanisms (Amin et al. 2016). In this method, the CAD model gets converted into a readable file—STL file, i.e., a list of the triangular face that passes to the rapid prototyping system to form the model. RP analyzes the readable file, chops model,

Table 1 Various membrane fabrication techniques with their benefits and drawbacks

Methods	Benefits	Drawbacks	Ref
Phase inversion	<ul style="list-style-type: none"> *Cheap *Stability *Film-forming is fast *Uniformly distributed thickness 	<ul style="list-style-type: none"> *Non-uniformly distributed pore size *Limited to materials 	Dommati et al. (2019)
Electrospinning	<ul style="list-style-type: none"> *Cost of startup comparatively small *Mass production 	<ul style="list-style-type: none"> *Solvents used may be toxic *Non-uniformly distributed pore size *Weak mechanical stability *More time requiring 	Dommati et al. (2019)
Track etching	<ul style="list-style-type: none"> *Precise structure *Control over the shape and size of pores 	<ul style="list-style-type: none"> *Cost extensive *Poor reproducibility 	*Apel (2001)
3D printing	<ul style="list-style-type: none"> *Cost efficiency *Ease of operation *Design of complex structures *Production in a single step *Control over structures *Flexibility *Risk mitigation Sustainable *Chemical and mechanical stability *Material wastage is low 	<ul style="list-style-type: none"> *Time required for printing is more (post-processing) *Limitation in raw materials *Restrictions in build size *Delamination between layers may occur 	Wong and Hernandez (2012), Zhakeyev et al. (2017), and Ngo et al. (2018)

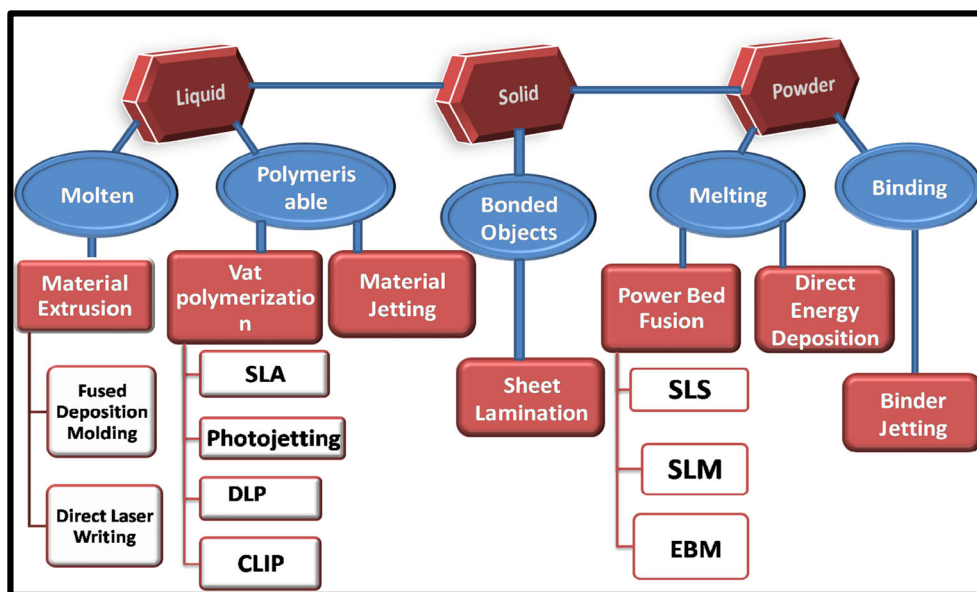
and craft assistance for the building process as the final point post-processing happens. The first 3D-printing technology by an additive process in which ultraviolet (UV) light hardens the polymer and create solid objects is introduced by the Japanese inventor Hideo Kodama (Dommati et al. 2019). 3DP is also known by different names like additive processes, rapid prototyping, additive fabrication, layer fabrication, and solid freeform fabrication (Guo and Leu 2013). Traditional techniques like mechanization, molding, and pressing contrive materials by effacing objects from massive stocks, whereas AM forges the ultimate form by appending objects, thereby making proper use of feedstock and generate minimized waste, reaching a middling geometrical accuracy (Kruth et al. 1998; Levy et al. 2003). The majority of germane AM technologies usually uses powder or wire as feedstock, selectively melted by the heat source, and fortified in ensuing cooling to form a part (Dirk Herzog et al. 2016). 3DP shows increased flexibility, enables low-cost volume production, and fabricates almost any geometrically complex shapes. AM technology reformed the prototyping industries that formerly count on posh and time-consumed methods such as molding and mechanization. 3DP is termed as rapid prototyping (RP) due to its widespread applications in the creation of prototypes (Balogun et al. 2019). The applications of 3D printing comprise product design, manufacturing, architecture, medical, and pharmaceutical sector (Hwa et al. 2018). Several AM techniques are present for various materials, and they are categorized into seven processes. Figure 1 shows the different types in 3DP: powder bed fusion, vat photopolymerization, direct energy deposition, binder jet printing, material jetting,

and fused filament fabrication. Another method of categorizing is based upon the starting material, whether solid-, liquid-, and powder-based printers (Lee et al. 2016b). Various AM methods evince various processing parameters that include manufacturing speed, mechanical strength, resolution, and surface finish that partially depend on the type and state of materials used (Dommati et al. 2019).

3DP of foams, scaffolds, membranes, etc. have a comprehensive array of utilization in depuration of water where toxic pollutants penetrate the human body through the food chain, thus affecting manifold of organs like the brain, heart, kidney, lungs, liver, and skin, inducing cancers, allergies, dysfunction of organs, etc. Among the membranes, foams, and scaffolds, the semi-permeable and poriferous property of membranes make them a potential candidate for water treatment by which the heavy metals, dyes, oils, pharmaceuticals, etc. can be removed to an extent. 3D printing of membranes has advantages of controlling pore size, thereby showing complete removal of noxious substances.

AM endow with more considerable attention towards devising the segregation of membrane and subjected to fabricating parts of different sizes from small to large scale, offers novel membrane grounding techniques that can fabricate membrane of diverse sizes and shapes that cannot be fashioned with traditional methods like phase inversion. Membrane module manufacturing in 3D from material to module monitored in single operation improves membrane segregation at both material and processing levels (Low et al. 2017). The problems encountered during water purification, such as pressure drop, concentration gradient, soiling,

Fig. 1 Types in 3DP



and low material transferring, were extinguished by the introduction of 3D printing (Balogun et al. 2019).

Fabrication of membrane by 3DP techniques

3DP has a wide range of applications in various fields and is still in the run in the field of membrane engineering. The configuration of membranes using traditional methods is limited to flat, hollow, or tube-like structures and here arises the relevance of 3DP techniques that can design almost any complicated geometrical shapes that can be dreamed of. The different types of 3D printers available can design membranes according to any shapes and available materials with less time consumption. Table 2 discusses the classification of various 3DP technologies along with their advantages, disadvantages, and resolution ranges.

Powder bed fusion technology

An AM process where laser stimulates incomplete or complete fusing within powdered particulate causing sintering or melting accompanied by a roller that affixes and smoothens another powdered layer, the process continues until the design forms (Kruth et al. 2005) and is shown in Fig. 2.

The solid- or liquid-based powder bed fusion technology (PBF) determines the porosity of 3D-printed parts, so, the preparatory material decides the type of technology suitable for modeling of RO membranes (Lee et al. 2016a). In solids, sintering results in the blending of materials at the surface, causing natural porosity of part while in liquids, complete melting of materials occurs, resulting in the formation of dense part with no porosity. Selective laser sintering (Yap

et al. 2015, 2016), selective laser melting, and electron beam melting (Kok et al. 2016) are the focal examples of PBF.

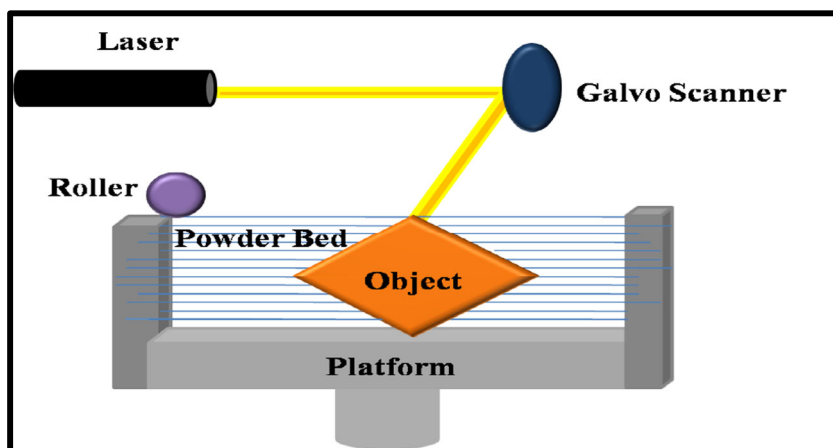
Powdered glass, plastic, metal, or ceramic used as printing materials in SLS, deposit at the print surface as thin coating, and highly powered laser selectively fuse these materials, thus making it easier to draw into layers. The laser fuses the powdered particulates to create a solidified layer, thereby moving along the x - and y -axis to the pattern by CAD data. Build tray moves down with fusion of the first layer, and after that, deposition and sintering of a new-fangled powdered layer occurs. Alternating deposition and platform lowering enable the distribution of a large amount of powder for build formation. Printing progresses at the inert atmosphere (Kruth et al. 2005) to avert any undesirable action. On manufacture completion, the opaque, abrasive, and porous prototype detaches from the tray; contiguous unsintered powder serves as a backup for the build and is dusted off later, and surface finishing is done by sandblasting (Berry et al. 1997). Prior production of hot melt-extruded filaments is not required and produces laser precision high-resolution objects.

SLM processes powdered materials with an intensified laser that entirely melt and fuse the material into a compactly consolidated structure with elevation in properties compared with bulk materials, manufactured in a layer-wise manner direct from the CAD data (Louvis et al. 2011). Allowing the spread of new-fangled powder, printing continues until the design reaches completion. High density avoids extensive post-processing as requisite with metal powders in SLS. SLM is more challenging to handle due to high-intensity laser and the problems faced during the fully melting of particle-like residual stresses, balling, and deformation (Kruth et al. 2004). High resolution, resource efficiency, good part design, and production flexibility result in wide-scale applications of SLM (Tan et al. 2018).

Table 2 Differentiation of 3D process along with their principle, pros, cons, and resolution range

3DP process	Principle	Pros	Cons	Resolution range	Ref.
Stereolithography (SLA)	Selective cure of resin with UV	<ul style="list-style-type: none"> *Able to imprint complex structures *Resolution is high *Strong precision 	<ul style="list-style-type: none"> *Need support systems *Slow *Material limitation 	10 μm	Chua et al. (1998) and Low et al. (2017)
Digital light processing (DLP)	Layer-wise curing with photopolymers	<ul style="list-style-type: none"> *Fast printing *Superior laying accuracy *Low printing costs 	<ul style="list-style-type: none"> *High cost *Build size is small *Poorer mechanical characteristics 	15–150 μm	Low et al. (2017)
Continuous liquid interface production (CLIP)	Photopolymerization with oxygen deficiency to generate a continuous liquid interface between the growing segment and the exposure window.	<ul style="list-style-type: none"> *High-speed printing *Layer less *Wide variety of materials and colors, using polymer 	<ul style="list-style-type: none"> *Build size is small 	50 μm	Low et al. (2017)
Fused deposition modeling (FDM)	Flash single image of each layer at once	<ul style="list-style-type: none"> *Cost is low *Vast array of raw materials *Versatile *Speed is high 	<ul style="list-style-type: none"> *Need for support systems *Mechanical properties are weak 	50–200 μm	Low et al. (2017) and Ngo et al. (2018)
Material jetting	UV-curable resins resulting in solidification of layers at once	<ul style="list-style-type: none"> *Resolution is high *Variety of materials and colors *High accuracy 	<ul style="list-style-type: none"> *Cost is high *Photosensitive *Poorer mechanical properties *Need for post--processing 	16 μm	Lee et al. (2017)
Selective laser sintering (SLS)	Localized powder melting	<ul style="list-style-type: none"> *Support systems are not needed *Fine resolution *Accuracy 	<ul style="list-style-type: none"> *High cost *Slow *Highly porous *Surface finishing is poor *Waste generation is high 	80–250 μm	Lee et al. (2017), Ngo et al. (2018), and Rastogi and Kandasubramanian (2019a)
Selective laser melting (SLM)	Localized powder melting	<ul style="list-style-type: none"> *No geometrical restrictions *Low cost *Better accuracy and mechanical properties 	<ul style="list-style-type: none"> *Rough surface finish *Need of post--processing 	80–250 μm	Lee et al. (2017)
Direct energy deposition	The material in the form of powder or wire melted by beam or laser	<ul style="list-style-type: none"> *Less time *Low cost *Mechanical properties are excellent 	<ul style="list-style-type: none"> *Need for support systems *Surface finish is poor 	250 μm	Ngo et al. (2018)
Binder jetting	The liquid binding agent is deposited selectively for joining powder particles	<ul style="list-style-type: none"> *Low cost *No support systems *Economic *Fast 	<ul style="list-style-type: none"> *Less accurate *Poor mechanical properties 	35 μm	Low et al. (2017)

Fig. 2 Powder bed fusion



The notable difference between SLS and SLM is that in SLM, the materials to be printed are wholly melted and have higher energy sources while in SLS, restricted melting occurs. In electron beam melting (EBM), the inclusive melt of powdery print materials occurs by liberation of high-voltage electrons typically 30 to 60 kV from an electron gun. To avoid oxidation, the process occurs in a high vacuum chamber (Wong and Hernandez 2012). Once electrons liberate, they focused on electromagnetic lenses that ensure liquefying of powdered material into structures predetermined by CAD design. When one layer forms, the powdered matter gets rolled onto the bed, and the method continued until the final object is modeled (Balogun et al. 2019). EBM also processes a vast array of pre-alloyed metals. This process in the future can be used in manufacturing in outer space, as it makes use of a high vacuum chamber. In the PDF process, the specific energy per volume of each scan (W) is a function of process parameters like scan speed (v), power of the laser (P), hatch distance (h), and layer thickness or Z-increment (t).

$$W = \frac{P}{v \times h \times t} \quad (3)$$

Also, the sinter energy per unit area (Ws') is required to amplify the mass of powdered materials beyond the T_g expressed as

$$Ws' = \rho c l_1 \delta T \quad (4)$$

ρ is the density of used powder, c is the specific heat capacity, l_1 is the total thickness of the un-sintered layer, and δT is the rise of ambient temperature to polymer-sintered temperature (Lee et al. 2017).

Binder jetting

A binder usually liquid is inkjet printed to a powder that spreads onto a bed, and a 3D part is developed by sticking particles together resulting in layer-wise manufacture of the

proposed CAD model and later shaken to remove it from the bed and then sintered, the eminence of the product is limited by the volume of loutish powder needed in the rolling step (Balogun et al. 2019). Figure 3 shows a binder jetting 3D printer. The fringe benefit of the binder jetting technique includes hefty build volume, free of support, high print speed, design freedom, and relatively low cost. Granular-formed metals, sand, and ceramics are commonly used materials in binder jetting with applications including the manufacture of **hefty sand molds, full-color prototypes**, and affordable 3D print metal parts. The advantage of binder jetting concerning other 3D printing techniques is that bonding occurs at **room temperature**, so that dimensional distortions such as warping in fused deposition modeling (FDM), SLS, or curling in SLA/DLP due to thermal effects are not a predicament in binder jetting. Another difference of binder jet is the absence of support structures where the surrounding powder provides all necessary support to the part, thus allowing the creation of free form metal structures. Other distinct features include a reduction in printing time, mishmash of powder, and binder enabling a wide range of material compositions, formation of slurries with higher solid loadings (Afshar-Mohajer et al. 2015).

The droplet energy (W_d) in the binder jetting (BJ) process is composed of surface energy and kinetic energy

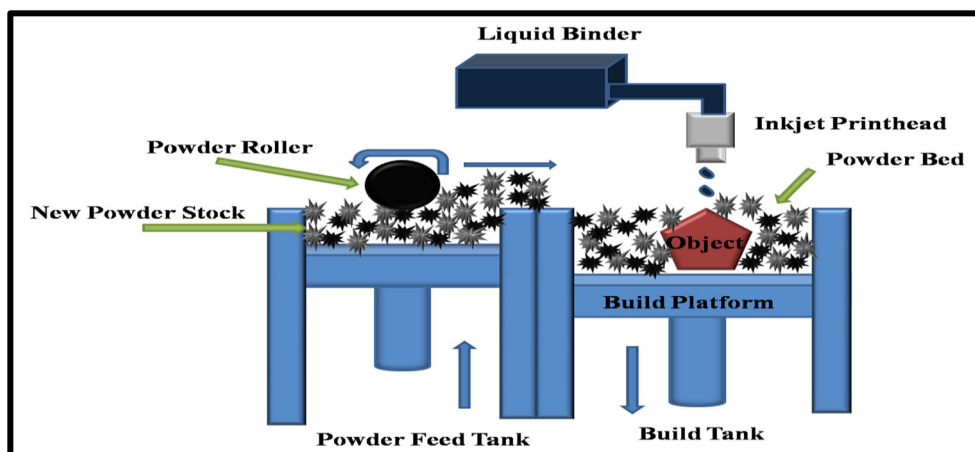
$$W_d = \sigma \pi d_d^2 + \frac{\rho V_d v^2}{2} \quad (5)$$

The droplet energy per aggregate volume is associated with the droplet given by adhesive binding energy (W^*)

$$W^* = \sigma \pi d_d^2 + \frac{\sigma \pi d_d^2}{V_a} + \frac{\rho V_d v^2}{V_a} \quad (6)$$

here, V_a is the aggregate volume expressed as

Fig. 3 Binder jetting



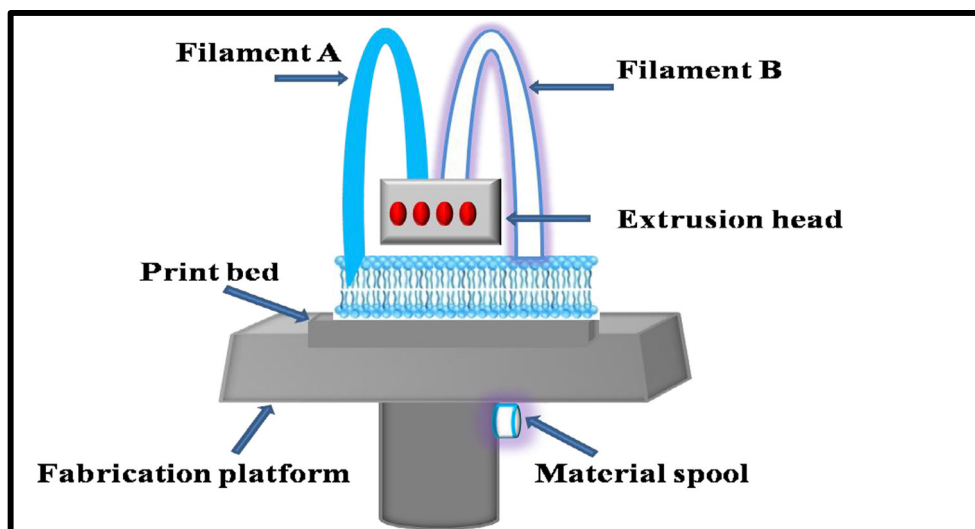
$$V_a = \frac{\pi}{6(kd_d)^3} \tag{7}$$

where K is constant and d_d is droplet diameter (Lee et al. 2017).

Material extrusion

In material extrusion, once constant pressure is applied, the material turf out using a printing head and at a constant speed, the material that extrudes set down and get solidified on the substratum; continuation of the process occurs until final prototype and shown in Fig. 4. This type of 3DP includes FDM and direct laser writing (DLW) (Balogun et al. 2019). In FDM, thermoplastic polymer filament feed material is heated above its glass transition temperature (T_g) and extrudes through a print head that moves in X–Y plane forming 3D structure by addition of layers (Gnanasekaran et al. 2017) on the print surface, instantly solidifying under controlled temperature, accompanied by layer assembly forming 3D

Fig. 4 Material extrusion



geometry. In the case of DLW, laser exposes photo-resisting resin to two-photon polymerization that can straightaway print clearly defined poriferous membrane with pore size up to 500 nm (Balogun et al. 2019).

The specific energy for incompressible melt flows by FDM process is (Eq. 8):

$$\rho c_p \left(\frac{dT}{dt} + (\vec{v} \cdot \nabla) T \right) = -\nabla_q \cdot (\vec{\tau} : \nabla \vec{v}) + \emptyset \tag{8}$$

where ρ is density, p is applied pressure, τ is surface force, T is temperature, v is velocity, \emptyset is change in internal energy due to heat source, and ∇_q is change in energy per unit time and volume due to heat conduction.

Vat photopolymerization

Vat photopolymerization is mostly marked for the fabrication of membranes where selective vat curing of photopolymer occurs by light as a source, which includes digital light processing (DLP), stereolithography (SLA), photopolymer

jetting, and continuous liquid interface production (CLIP) and shown in Fig. 5. In SLA, the surface of the photo-curable resin is selectively exposed to fine scanning laser showing vector form projection undergoing photo-polymerization reaction that comprises photo-initiators, reactive monomers, and additives and thereby becomes solid. In DLP, they make use of the DLP projector instead of UV laser for projecting overall transversal layers of 3D structures with the upward movement of platform in printing, although the downward movement is possible as well.

In VP, the specific energy (W^*) describes the photo-activation of photopolymer (Eq. 9):

$$W^* = \frac{W'_c}{l_c} \exp\left(\frac{l_c}{l_p}\right) \quad (9)$$

where W'_c is the threshold curing for photopolymer resin transition, l_c is the depth of curing, and l_p is the penetration depth.

Direct energy deposition

A high-intensity laser focused on a small region causes the substrate to heat, thereby melting print materials. Rather than pre-deposition, the continuous stream of powder material to substrate happens in direct energy deposition, as shown in Fig. 6. The energy source and rate of powder melt deposited influence the degree of resolution (Balogun et al. 2019). The resolution is high for energy source from laser than from beam while the lowest resolution due to heat input is for arc and fabrication speed depends on the rate of deposition

The absorption of laser energy (W_a) by the material is given by (Eq. 10)

$$W_a = AP_L t_i \quad (10)$$

where A is the heat absorbcency of laser on the surface of the metal, P_L is the power of the laser, t_i is the interaction time of the laser on the build platform. The interaction time is shown by (Eq. 11):

$$t_i = \frac{d}{v} \quad (11)$$

where d is the diameter of the laser and v is the laser scanning speed (Lee et al. 2017).

Material jetting

The method in material jetting uses the principle of customary paper printing (Balogun et al. 2019) based on the deposition of liquid droplets, i.e., light-curable resin on build platform that softens the previous layer, thereby solidifying together. Figure 7 shows the material jetting process that makes use of thin nozzles to extrude in a controlled manner, either molten material or a binder, to bind the powder in a solid object (Bikas et al. 2016). When layer-by-layer deposition is complete, it gets removed from the working platform, and then support material is removed. This technique is appropriate for modeling of polymeric sheet membranes and is useful in innovatory membrane fabrication. The printing technology produces not only prototypes but also functional polymeric components such as lightweight honeycombs, anatomical models, lifestyle wearable products, and scaffolds for tissue engineering (Yap et al. 2017).

3D-printed membranes in water treatment

The production of membranes includes 30% recycled and 70% virgin powder. Conventional membranes are mainly formed by solvent casting in which prepared solution passed on to a mold where it is oven dried, later followed by evaporation to confiscate enduring solvents. Complete dried membranes obtained are then engraved into preferred forms. 3D-printed membranes are used in water treatment because it upgrades some limitations of membranes like lack of reliability, slow operation, reduced selectivity, and elevated cost.

Fig. 5 Vat photopolymerization

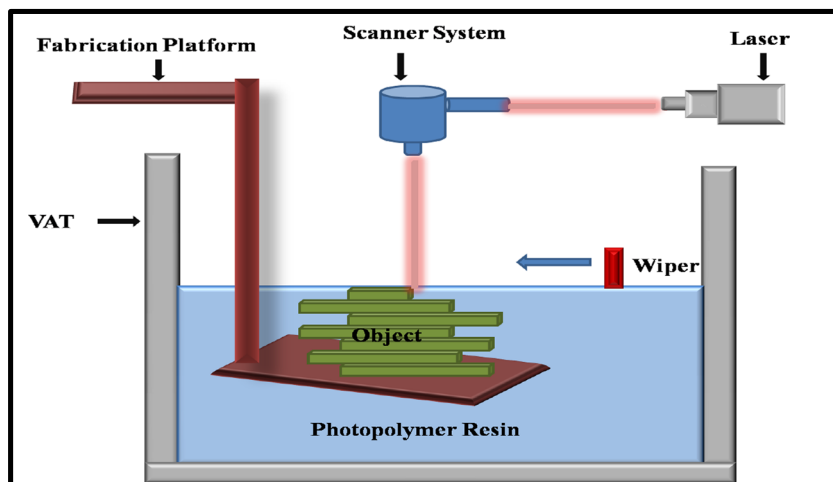
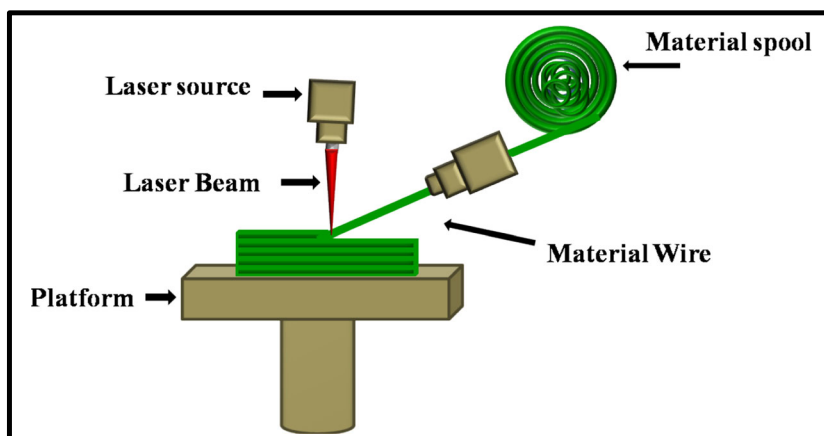


Fig. 6 Direct energy deposition



Primarily used membranes are polymeric membranes; many others include ceramics, metals, and alloys. The advancement of 3DP resulted in a low-power-consuming simple decisive tailor-made ecologically innocuous membranes with low solvent content having accelerated water discharge rate for smooth regulation of clog. A comparative study on some of the 3D-printed membranes along with their fabrication techniques, efficiency, membrane resistance, and operation conditions are shown in Table 3.

Yuan et al. (2015) conflated PA microfiltration membranes by SLS technique that had a far-reaching impact on the structure of membranes. Parameters that impact the input energy throughout membrane assemblage are laser power, scanning count, and hatch space. Membrane erected with higher laser power, reduced HS, and 2 counts have tiny pore size and thicker structure, thus engendering reduced permittivity for water. In contrast with conventional membranes developed by phase separation, the SLS membranes have comparatively low porosity (Yuan et al. 2015), mostly because the part among pores are dense in place of porous. When the ED is 0.1 J mm^{-2} , the PA membrane displayed an enticing rejection (Yuan et al. 2017a; Chowdhury et al. 2018). To achieve super-hydrophobicity, Yuan et al. (2017a) coated PA membranes with zeolitic imidazolate framework ZIF-L which was then modified using polydimethylsiloxane. The PDMS-ZIFL-PA

membrane showed super-hydrophobic and super-oleophilic characters which were useful in oil-water separations during the treatment of oily sewages or chemical discharges in water thereby allowing the permeation of oil through it (Fig. 8a). Membrane performance (Fig. 8b, c) was studied through the rejection and flux of various oils such as hexane, mineral oils, heptanes, and petroleum ethers in which all the oils showed about 99% rejection and $24,000 \text{ L (m}^2 \text{ h)}^{-1}$ oil flux (Yuan et al. 2019).

The second 3DP PSU membrane conflated by Yuan et al. (2017b) using SLS comprise densely fritted layers and pored mid-layer composed of partially frit PSU powders with 15 W laser power, 0.15 mm HS, and 1 scan count. 3D-printed PSU membranes had broader pores, reason that viscosity of amorphous PSU particles is more substantial, resulting in a worse coalition and broader cavities. The membrane had a hydrophobic base with contact angle 124° and top with 89° . PSU membrane, when submerged for 4 min in candle soot, the water contact angle increased drastically to 141° , proving substantial amelioration of candle soot to the hydrophobicity of the membrane surface. Further, when submersion time rises to 20 min, the membrane evinced a super-hydrophobic surface with 155° contact. Membrane, aside from its super-hydrophobicity characteristics with contact angle of 161° and slide angle of 5° , showed super-oleophobic characters.

Fig. 7 Material jetting

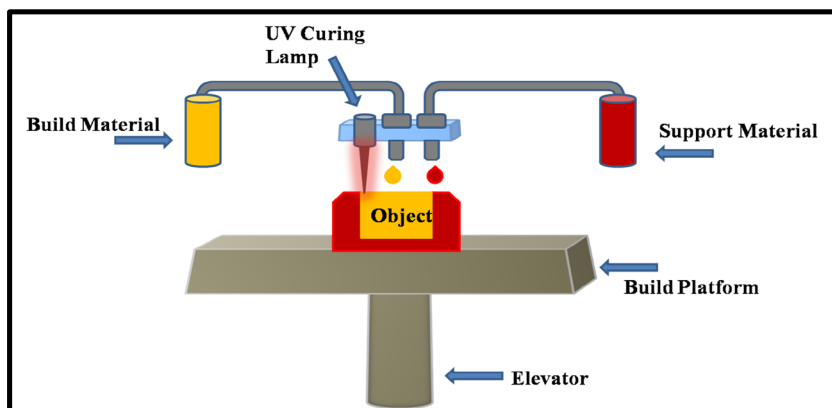


Table 3 Comparative study of various 3D membranes

Material	Section printed in 3D	Process	Efficiency	Operating conditions	Membrane resistance	Particulars	Ref.
Acrylonitrile butadiene styrene and polyethersulfone	Wavy 3D composite membrane	Multijet printing	87% permeance	Transmembrane pressure = 1 bar and Reynolds number = 400, 800, 1000	96% bovine serum albumin rejection	*Effective filtration due to wavy structure *Chemical free *Oil rejection *Anti fouling behavior	Mazinani et al. (2019)
Fluorine containing diamine and m-phenylenediamine-based polyamide	Patterned thin film composite membrane	Inkjet printing and interfacial polymerization	1.26 ± 0.06 LMH/bar average permeability	27 bar transmembrane pressure and temperature 25°C	97.9% salt rejection	*Enhanced ion or compound separation	Badalov et al. (2015)
Nanosilica-filled polydimethylsiloxane ink	Porous membrane	Homemade 3D printer	Flux = 23700 L m ⁻² h ⁻¹	NA	99.6% oil removal	*Weak interface adhesion is avoided *Super-hydrophobicity *Excellent mechanical stability *Separation of oils and corrosives	Lv et al. (2017)
Powder of Kankara clay and maltodextrin	Porous ceramic membrane	A-Z corporation 3D printer	The pores of the membrane were fairly large because of the rough particles, and the filtration efficiency is far greater	Pressure of 0.5 MPa	97.78% reduction in COD and 53.85% reduction in TSS (75 μm)	*Increase in water absorption due to interconnected network like densely packed structure	Hwa et al. (2018)
Polyethersulfone membrane and antimicrobial peptide	Foul-resistant membranes	Inkjet	48% reduction in flux is given	NA	*66% reduction of biovolume *32% reduction of average thickness *Bacterial inhibition of 36%	*Antibacterial surface development *Decreased growth of biofilms *Less cleaning *Long lasting *Reduce extra-energy cost	Mohanraj et al. (2018)

When oil drop contacts membrane surface, it disseminated over the said surface and imbued in a membrane within 1.5 s, insinuating a surface with super-oleophilic characters by forming candlesoot/oil layer (Fig. 9a). The soot-encrusted 3D print PSU membranes showed 99% separation efficiency for all oils and a flux rate of about 19,000 L (m² h)⁻¹ (Fig. 9b). Using water pre-wetted membrane results in the formation of candlesoot-water layer that separates water (dyed in red) from the oil-water mixture, thereby showing switchability of the membrane between hydrophobic and oleophobic characters (Fig. 9c). The stability of the switchable wettability of membrane was assessed using 10 cycles of oil-water separations (Fig. 9d) (Yuan et al. 2017b).

Xing et al. designed a poly(lactic acid) poriferous membrane having a superhydrophobic demeanor with coveted shape and porosity, forged using FDM that induces an ultra-high water adherence (380 μN) (Xing et al. 2018). PLA, a biologically compatible and biodegrading polyester that emanates renewable resources, is one among the several synthetic polymers assented by the Food and Drug Administration

(FDA) (Rasal et al. 2010). PLA membrane was modeled by FDM with print speed of 50 mm s⁻¹ by cross-flanking filament layers vertically and then cleansed using deionized water and ethanol to evacuate dirt. Addition of PS nanospheres with a diameter of 100 nm resulted in the roughening of the surfaces thereby enhancing the hydrophobic property of the membrane. The ensuing superhydrophobic membrane was then treated for oil-water separations in which oil permeated through the membrane whereas water (dyed with CuSO₄) is repelled from the membrane due to its hydrophobicity. High permanence with increased mechanical and chemical properties resulted in the usage of 3D-print PLA membrane for severance of oil and corrosive aqueous solutions. Besides, the superhydrophobic membrane (porosity 250 μm) presented a high flux of 60 kL m⁻² h⁻¹ and efficiency of separation of 99.4% with an intrusion pressure of 1.76 kPa for mixtures of water and other alkane oils (Xing et al. 2018).

Nanosun introduced PVDF polymeric membrane by compressing the nanofibres produced in millions into an ultrathin sheet that would enlarge the surface area

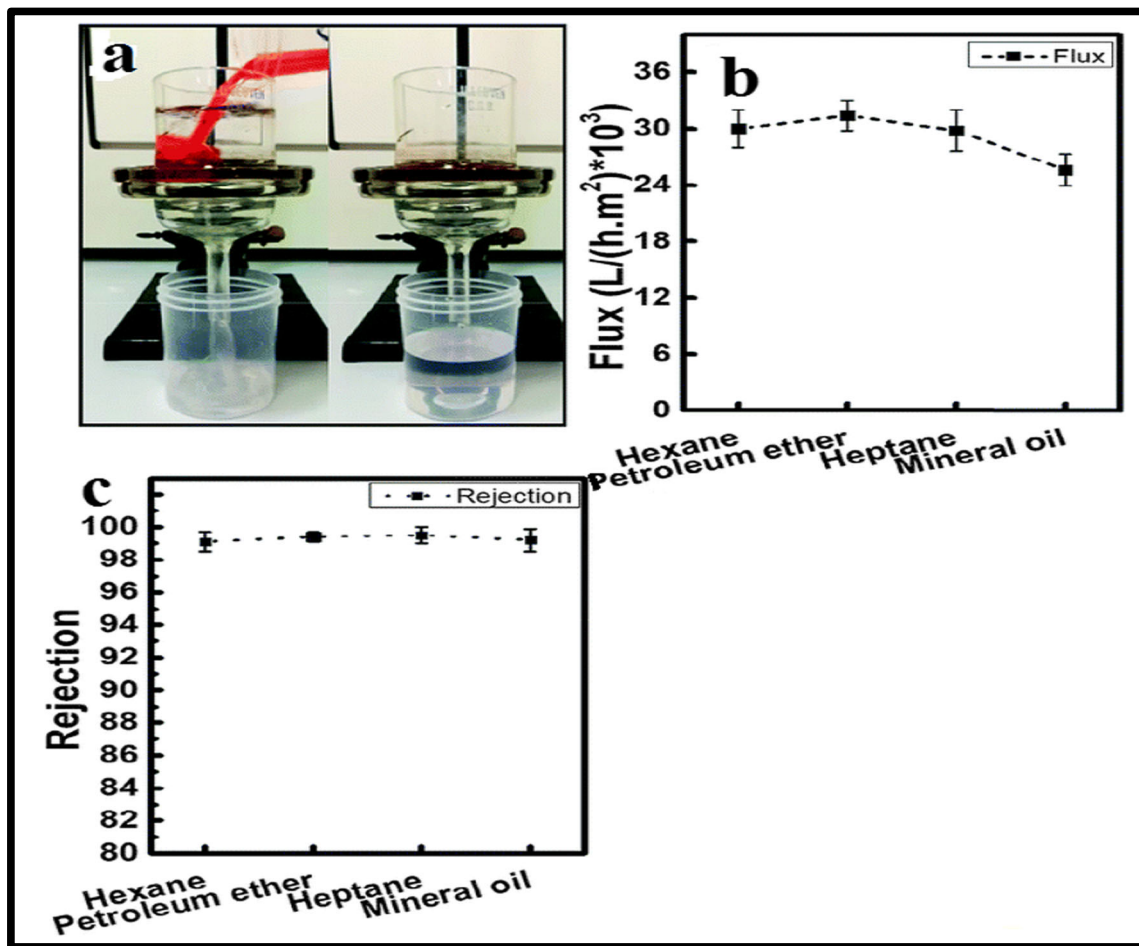


Fig. 8 PDMS-ZIFL-PA membrane showing: **a** oil separation from water, **b** flux of different oils, and **c** rejection of oils. Reprinted with permission from Yuan et al. (2019). Copyright 2019, Royal Society of Chemistry

allowing water runaway at a faster rate, thereby trapping the pollutants. Membranes were made into micro- or ultrafiltration membranes by adjusting the thickness of fibers stacked on one another.

Withell et al. (2011), using clay powder, manufactured 3D-printed ceramic membranes at quite affordable prices. The 3DP-created ceramic membrane that can be used to build complicated geometries has the strengths of using minimal materials, expenses, labor, and energy. The application of relatively cheap ceramic membranes having greater mechanical and chemical resistance than many polymer membranes offers an effective approach towards wastewater treatment (Withell et al. 2011). According to Dommati et al. (2019), printing of ceramic membrane allows sustainable membranes to be manufactured with an enhanced structure and higher performance than traditional membranes. The fabricated ceramic components appear to be superior in mechanical strength and are not reactive to foreign particles, which helps them to be more appropriate in interacting with bacteria-destroying agents thereby enhancing filtration. Majouli et al. (2011) showed that in an acid medium, the membranes have a greater

chemical resistance than in the base medium. The porous clay-based membrane was built specifically to extract harmful bacteria and other organic matters from water supplies (Majouli et al. 2011).

Fouling continues to be an unresolved issue that impedes pervasive industrial usage of membranes. 3D composite ultrafiltration membranes by combining polyether sulfone layer on a printed wavy or flat support proposed by Mazinani et al. (2019) were studied for anti-fouling behavior. The permeation performance of both flat and wavy membranes at an operation condition of 1000 *R_c* and 1 bar transmembrane pressure resulted in 10% higher permeation in wavy when compared with flat membranes thereby showing a lower deposition rate of bovine serum albumin in the wavy membrane. The enhanced performance of the wavy membrane is because of their 13% higher filtration areas than flat, which is an advantage for their antifouling behavior that helps them to attain 87% permeance and a BSA rejection of 96% (Mazinani et al. 2019).

Badalov et al. (2015) studied the hybridization of 3DP technology and interfacial polymerization by making thin-film composite membranes by inserting fluorine-containing

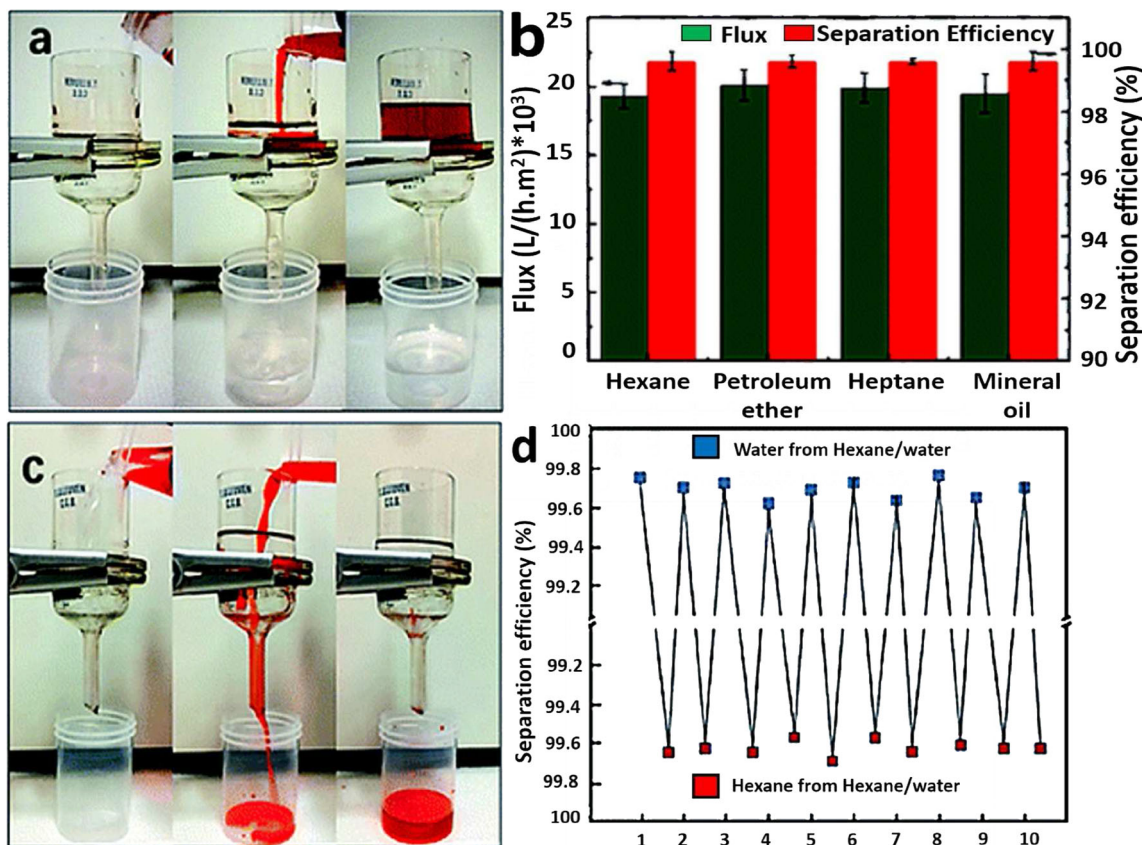


Fig. 9 Performance of 3D-printed PSU membrane. **a** Oil separated from oil/water mixture (water is marked using red dye). **b** Efficiency of separation and flux for different oils. **c** Water separated from oil/water

mixture. **d** Separation efficiency of water and oil (hexane) from hexane/water mixture in ten cycles. Reprinted with permission from Yuan et al. (2017b). Copyright 2017, Royal Society of Chemistry

diamine into *m*-phenylene diamine-based polyamide, which showed an upsurge in ion rejections and flux volume. Permeability of the membrane (L_p) (Eq. 12) was calculated by

$$L_p = \frac{\Delta V}{A \times \Delta t \times \Delta P} \quad (12)$$

ΔV is the volume of permeate collected, A is the area of the membrane, Δt is the collection period of permeate, and ΔP is pressure. Rejection of salt (Eq. 13) is measured by

$$R\% = \left(1 - \frac{C_p}{C_f}\right) \times 100 \quad (13)$$

where C_p is the concentration of salt in permeate and C_f is the concentration of salt in feed (Badalov et al. 2015).

Developing enhanced water purification continues to be a critical component of water safety and conservation. While some 3DP techniques may pose fewer dilemmas, they are quite inadequate to encounter emerging traditional membrane manufacturing technologies so far. The main disadvantages entail the expense of 3DP membranes, infrastructure constraints, technological expertise and specifications, scalability, and existing financial

viability. The expense repercussions of 3DP membranes are on printer costs and material costs. Widely deployed 3D printers may not be so effective in developing desalination membranes so it is vital to need extremely robust 3D printers for membrane manufacturing with an acceptable printing budget that can cope with traditional techniques. Failure of the fused deposition-modeled membrane may occur due to layer delamination, thereby boosting the membrane substitution rate in the desalination processes and water purification. It is rather undesirable for industrial purposes, as large-volume membranes are complicated to print. This will also need skills in membrane technologies to diversify the 3DP techniques pertinent to membrane manufacturing (Melenka et al. 2016).

Given that 3DP is a comparatively new water purification technology, further assessments are needed to enhance its application and render it even more practical for water purification. Besides, the 3DP membranes probably had superior output in various applications as opposed to traditional ones. Researches on augmenting 3DP resolution, speed, and availability of materials are projected to raise its prominence in future water treatment.

Conclusion and future perspective

The unremitting advances in 3D printing have led to an increase in its application in the field of membrane technology. Membrane technology has engrossed immense attention as one of the most potential substitutes for traditional processes as a result of its high segregation efficiency, lower power consumption, easy control of membrane fouling, low investment, and environmental friendliness. The nanofibres formed are layered on top of each other in 3DP, forming a stack which is then compressed to form membranes. Membranes that contrive as hollow fibers or as flat sheets for purification purposes in conventional methods can be fabricated to any shapes using 3DP, thus enabling increased mass transfer. Another vital factor of 3DP is its ability to manufacture the entire membrane structure right from the module to spacer with distinct materials all at once, thus reducing production time. An Overall idea about toxicity of pollutants, membrane filtration, AM technology, membrane fabrication process, and its use in the treatment of water were discussed in this review. However, 3D-printed membranes were not fully able to encounter the problems faced during water treatment, so there is a need for future considerations. In future perspective, firstly, the notion of 4D printing can be brought about for effective membrane designing. Secondly, the incorporation of nature-inspired ideas could result in improving the strength and functions of models. Thirdly, the introduction of new materials or blends for fabricating membranes should result in a wide range of properties and applications of membranes. Moreover, future researches on the resolution and speed of 3D printing are expected to increase the bearing of membranes in water treatment.

Acknowledgments The authors are thankful to Dr. C. P. Ramanarayanan, Vice-Chancellor of DIAT (DU), Pune for the motivation and support. The first author would like to acknowledge Dr. B. Srinivasulu, Principal Director and Head, CIPET: Institute of Plastic Technology (IPT), Kochi, for the support. The authors are thankful to Mr. Raviprakash Magisetty, Mr. Prakash M. Gore, Mr. Swaroop Gharde, and Ms. Alsha Subash for their persistent technical support throughout the review writing. The authors are thankful to all anonymous reviewers and the Editor for improving the quality of the revised manuscript by their valuable suggestions and comments.

References

- Afshar-Mohajer N, Wu C-Y, Ladun T et al (2015) Characterization of particulate matters and total VOC emissions from a binder jetting 3D printer. *Build Environ* 93:293–301. <https://doi.org/10.1016/j.buildenv.2015.07.013>
- Alaimo G, Marconi S, Costato L, Auricchio F (2017) Influence of meso-structure and chemical composition on FDM 3D-printed parts. *Compos Part B Eng* 113:371–380. <https://doi.org/10.1016/j.compositesb.2017.01.019>
- Amin R, Knowlton S, Hart A et al (2016) 3D-printed microfluidic devices. *Biofabrication* 8:1–16. <https://doi.org/10.1088/1758-5090/8/2/022001>
- Amjad Z (1993) Reverse osmosis : membrane technology, water chemistry & industrial applications. Van Nostrand Reinhold, New York
- Apel P (2001) Track etching technique in membrane technology. *Radiat Meas* 34:559–566. [https://doi.org/10.1016/S1350-4487\(01\)00228-1](https://doi.org/10.1016/S1350-4487(01)00228-1)
- Arora R, Singh N, Balasubramanian K, Alegaonkar P (2014) Electroless nickel coated nano-clay for electrolytic removal of Hg(II) ions. *RSC Adv* 4:50614–50623. <https://doi.org/10.1039/c4ra06988a>
- Badalov S, Oren Y, Arnusch CJ (2015) Ink-jet printing assisted fabrication of patterned thin film composite membranes. *J Membr Sci* 493: 508–514. <https://doi.org/10.1016/j.memsci.2015.06.051>
- Balogun HA, Sulaiman R, Marzouk SS et al (2019) 3D printing and surface imprinting technologies for water treatment: a review. *J Water Process Eng* 31:100786. <https://doi.org/10.1016/j.jwpe.2019.100786>
- Becquer T, Quantin C, Sicot M, Boudot J (2003) Chromium availability in ultramafic soils from New Caledonia. *Sci Total Environ* 301:251–261. [https://doi.org/10.1016/S0048-9697\(02\)00298-X](https://doi.org/10.1016/S0048-9697(02)00298-X)
- Berlin M, Zalups RK, Fowler BA (2015) Mercury. In: *Handbook on the toxicology of metals*. Elsevier, pp 1013–1075
- Berman B (2012) 3-D printing: the new industrial revolution. *Bus Horiz* 55:155–162. <https://doi.org/10.1016/j.bushor.2011.11.003>
- Bernhoft RA (2012) Mercury toxicity and treatment: a review of the literature. *J Environ Public Health* 2012:1–10. <https://doi.org/10.1155/2012/460508>
- Berry E, Brown JM, Connell M et al (1997) Preliminary experience with medical applications of rapid prototyping by selective laser sintering. *Med Eng Phys* 19:90–96. [https://doi.org/10.1016/S1350-4533\(96\)00039-2](https://doi.org/10.1016/S1350-4533(96)00039-2)
- Bhalara PD, Punetha D, Balasubramanian K (2014) A review of potential remediation techniques for uranium(VI) ion retrieval from contaminated aqueous environment. *J Environ Chem Eng* 2:1621–1634. <https://doi.org/10.1016/j.jece.2014.06.007>
- Bikas H, Stavropoulos P, Chryssolouris G (2016) Additive manufacturing methods and modelling approaches: a critical review. *Int J Adv Manuf Technol* 83:389–405. <https://doi.org/10.1007/s00170-015-7576-2>
- Bui N-N, Arena JT, McCutcheon JR (2015) Proper accounting of mass transfer resistances in forward osmosis: improving the accuracy of model predictions of structural parameter. *J Membr Sci* 492:289–302. <https://doi.org/10.1016/j.memsci.2015.02.001>
- Chowdhury MR, Steffes J, Huey BD, McCutcheon JR (2018) 3D printed polyamide membranes for desalination. *Science* (80-) 361:682–686. <https://doi.org/10.1126/science.aar2122>
- Chua CK, Chou SM, Wong TS (1998) A study of the state-of-the-art rapid prototyping technologies. *Int J Adv Manuf Technol* 14:146–152. <https://doi.org/10.1007/BF01322222>
- Chua CK, Yeong WY, An J (2017) 3D Printing and Bioprinting in MEMS Technology. *Micromachines* 8:229. <https://doi.org/10.3390/mi8070229>
- Davis A, Balasubramanian K (2016) Bioactive hybrid composite membrane with enhanced antimicrobial properties for biomedical applications. *Def Sci J* 66:434–438. <https://doi.org/10.14429/dsj.66.10218>
- Deoray N, Kandasubramanian B (2018) Review on three-dimensionally emulated fiber-embedded lactic acid polymer composites: opportunities in engineering sector. *Polym-Plast Technol Eng* 57:860–874. <https://doi.org/10.1080/03602559.2017.1354226>
- Dommati H, Ray SS, Wang J-C, Chen S-S (2019) A comprehensive review of recent developments in 3D printing technique for ceramic membrane fabrication for water purification. *RSC Adv* 9:16869–16883. <https://doi.org/10.1039/C9RA00872A>
- Farrell WJ, Peggy OD, Colklin M (2001) Electrochemical and spectroscopic study of arsenate removal from water using zero-valent iron media. *Environ Sci Technol* 35(10):2026–2032

- Ferguson JF, Gavis J (1972) A review of the arsenic cycle in natural waters. *Water Res* 6:1259–1274. [https://doi.org/10.1016/0043-1354\(72\)90052-8](https://doi.org/10.1016/0043-1354(72)90052-8)
- Gautam RK, Sharma SK, Mahiya SCM (2014) Contamination of heavy metals in aquatic media: transport, toxicity, and technologies for remediation. In: Sharma S (ed) *Heavy metals in water: presence, removal and safety*. The Royal Society of Chemistry, pp 1–24
- Gautam A, Gore PM, Kandasubramanian B (2020) Nanocluster materials in photosynthetic machines. *Chem Eng J* 385:123951. <https://doi.org/10.1016/j.cej.2019.123951>
- Gharde S, Goud R, Nimje S, Kandasubramanian B (2019a) 6. Aggrandized flexural properties of assorted natural biological materials. In: Kumar K, Davim JP (eds) *Biodegradable composites*. De Gruyter, Berlin, pp 111–140
- Gharde S, Surendren A, Korde JM et al (2019b) Recent advances in additive manufacturing of bio-inspired materials. In: *Biomufacturing*. Springer International Publishing, Cham, pp 35–68
- Gibson I, Rosen D, Stucker B (2015) *Additive manufacturing technologies*. Springer, New York, NY
- Giwa A, Akther N, Dufour V, Hasan SW (2016) A critical review on recent polymeric and nano-enhanced membranes for reverse osmosis. *RSC Adv* 6:8134–8163. <https://doi.org/10.1039/C5RA17221G>
- Gnanasekaran K, Heijmans T, van Bennekom S et al (2017) 3D printing of CNT- and graphene-based conductive polymer nanocomposites by fused deposition modeling. *Appl Mater Today* 9:21–28. <https://doi.org/10.1016/j.apmt.2017.04.003>
- Gonte RR, Balasubramanian K (2012) Chemically modified polymer beads for sorption of gold from waste gold solution. *J Hazard Mater* 217–218:447–451. <https://doi.org/10.1016/j.jhazmat.2012.03.020>
- Gonte RR, Balasubramanian K, Mumbreaker JD (2013) Porous and cross-linked cellulose beads for toxic metal ion removal: Hg(II) ions. *J Polym* 2013:1–9. <https://doi.org/10.1155/2013/309136>
- Gonte RR, Shelar G, Balasubramanian K (2014) Polymer–agro-waste composites for removal of Congo red dye from wastewater: adsorption isotherms and kinetics. *Desalin Water Treat* 52:7797–7811. <https://doi.org/10.1080/19443994.2013.833876>
- Gore PM, Kandasubramanian B (2018) Heterogeneous wettability cotton based superhydrophobic Janus biofabric engineered with PLA/functionalized-organoclay microfibers for efficient oil–water separation. *J Mater Chem A* 6:7457–7479. <https://doi.org/10.1039/C7TA11260B>
- Gore PM, Dhanshetty M, Kandasubramanian B (2016a) Bionic creation of nano-engineered Janus fabric for selective oil/organic solvent absorption. *RSC Adv* 6:111250–111260. <https://doi.org/10.1039/C6RA24106A>
- Gore PM, Zachariah S, Gupta P, Balasubramanian K (2016b) Multifunctional nano-engineered and bio-mimicking smart superhydrophobic reticulated ABS/fumed silica composite thin films with heat-sinking applications. *RSC Adv* 6:105180–105191. <https://doi.org/10.1039/c6ra16781k>
- Gore P, Khraisheh M, Kandasubramanian B (2018a) Nanofibers of resorcinol–formaldehyde for effective adsorption of As (III) ions from mimicked effluents. *Environ Sci Pollut Res* 25:11729–11745. <https://doi.org/10.1007/s11356-018-1304-z>
- Gore PM, Khurana L, Siddique S et al (2018b) Ion-imprinted electrospun nanofibers of chitosan/1-butyl-3-methylimidazolium tetrafluoroborate for the dynamic expulsion of thorium (IV) ions from mimicked effluents. *Environ Sci Pollut Res* 25:3320–3334. <https://doi.org/10.1007/s11356-017-0618-6>
- Gore PM, Naebe M, Wang X, Kandasubramanian B (2019a) Progress in silk materials for integrated water treatments: fabrication, modification and applications. *Chem Eng J* 374:437–470. <https://doi.org/10.1016/j.cej.2019.05.163>
- Gore PM, Naebe M, Wang X, Kandasubramanian B (2019b) Silk fibres exhibiting biodegradability & superhydrophobicity for recovery of petroleum oils from oily wastewater. *J Hazard Mater* 121823. <https://doi.org/10.1016/j.jhazmat.2019.121823>
- Gore PM, Purushothaman A, Naebe M et al (2019c) Nanotechnology for oil-water separation. In: *Advanced research in nanosciences for water technology*. Springer, Cham, pp 299–339. https://doi.org/10.1007/978-3-030-02381-2_14
- Guo N, Leu MC (2013) Additive manufacturing: technology, applications and research needs. *Front Mech Eng*:215–243
- Gupta P, Kandasubramanian B (2017) Directional fluid gating by Janus membranes with heterogeneous wetting properties for selective oil-water separation. *ACS Appl Mater Interfaces* 9:19102–19113. <https://doi.org/10.1021/acsami.7b03313>
- Gupta P, Lalalikar V, Kundu R, Balasubramanian K (2016) Recent advances in membrane based waste water treatment technology: a review. *Energy Environ Focus* 5:241–267. <https://doi.org/10.1166/eef.2016.1227>
- Herzog D, Seyda V, Wycisk E, Emmelmann C (2016) Additive manufacturing of metals. *Acta Mater* 117:371–392
- Hwa LC, Uday MB, Ahmad N et al (2018) Integration and fabrication of the cheap ceramic membrane through 3D printing technology. *Mater Today Commun* 15:134–142. <https://doi.org/10.1016/j.mtcomm.2018.02.029>
- Hyde J, MacNicol M, Odle A, Garcia-Rill E (2014) The use of three-dimensional printing to produce in vitro slice chambers. *J Neurosci Methods* 238:82–87. <https://doi.org/10.1016/j.jneumeth.2014.09.012>
- Ivanova O, Williams C, Campbell T (2013) Additive manufacturing (AM) and nanotechnology: promises and challenges. *Rapid Prototyp J* 19:353–364. <https://doi.org/10.1108/RPJ-12-2011-0127>
- Kalathil A, Raghavan A, Kandasubramanian B (2019) Polymer fuel cell based on polybenzimidazole membrane: a review. *Polym Technol Mater* 58:465–497. <https://doi.org/10.1080/03602559.2018.1482919>
- Kelly BC, Ikonomou MG, Blair JD et al (2007) Food web-specific biomagnification of persistent organic pollutants. *Science* (80-) 317:236–239. <https://doi.org/10.1126/science.1138275>
- Khanale M, Balasubramanian K (2016) Molecular simulation of geometrically optimized polyoxymethylene/poly (vinylalcohol) gel membrane for electroless scrubbing Ni(II) ions. *J Environ Chem Eng* 4: 434–439. <https://doi.org/10.1016/j.jece.2015.11.044>
- Kok YH, Tan XP, Loh NH et al (2016) Geometry dependence of microstructure and microhardness for selective electron beam-melted Ti–6Al–4V parts. *Virtual Phys Prototyp* 11:183–191. <https://doi.org/10.1080/17452759.2016.1210483>
- Korde JM, Balasubramanian K (2019) Naturally biomimicked smart shape memory hydrogels for biomedical functions. *Chem Eng J*: 122430. <https://doi.org/10.1016/j.cej.2019.122430>
- Korde JM, Shaikh M, Kandasubramanian B (2018) Bionic prototyping of honeycomb patterned polymer composite and its engineering application. *Polym-Plast Technol Eng*:1–17. <https://doi.org/10.1080/03602559.2018.1434667>
- Krishna MVB, Chandrasekaran K, Karunasagar D, Arunachalam J (2001) A combined treatment approach using Fenton’s reagent and zero valent iron for the removal of arsenic from drinking water. *J Hazard Mater* 84:229–240. [https://doi.org/10.1016/S0304-3894\(01\)00205-9](https://doi.org/10.1016/S0304-3894(01)00205-9)
- Kruth J-P, Leu MC, Nakagawa T (1998) Progress in additive manufacturing and rapid prototyping. *CIRP Ann* 47:525–540. [https://doi.org/10.1016/S0007-8506\(07\)63240-5](https://doi.org/10.1016/S0007-8506(07)63240-5)
- Kruth JP, Froyen L, Van Vaerenbergh J et al (2004) Selective laser melting of iron-based powder. *J Mater Process Technol* 149:616–622. <https://doi.org/10.1016/j.jmatprotec.2003.11.051>

- Kruth J, Mercelis P, Van Vaerenbergh J et al (2005) Binding mechanisms in selective laser sintering and selective laser melting. *Rapid Prototyp J* 11:26–36. <https://doi.org/10.1108/13552540510573365>
- Lee J-Y, An J, Chua CK, et al (2016a) A perspective on 3D printed membrane: direct/indirect fabrication methods via direct laser writing
- Lee J-Y, Tan WS, An J et al (2016b) The potential to enhance membrane module design with 3D printing technology. *J Membr Sci* 499:480–490. <https://doi.org/10.1016/j.memsci.2015.11.008>
- Lee J-Y, An J, Chua CK (2017) Fundamentals and applications of 3D printing for novel materials. *Appl Mater Today* 7:120–133. <https://doi.org/10.1016/j.apmt.2017.02.004>
- Levy GN, Schindel R, Kruth JP (2003) Rapid manufacturing and rapid tooling with layer manufacturing (LM) technologies, state of the art and future perspectives. *CIRP Ann* 52:589–609. [https://doi.org/10.1016/S0007-8506\(07\)60206-6](https://doi.org/10.1016/S0007-8506(07)60206-6)
- Louvissier E, Fox P, Sutcliffe CJ (2011) Selective laser melting of aluminium components. *J Mater Process Technol* 211:275–284. <https://doi.org/10.1016/j.jmatprotec.2010.09.019>
- Low Z-X, Chua YT, Ray BM et al (2017) Perspective on 3D printing of separation membranes and comparison to related unconventional fabrication techniques. *J Membr Sci* 523:596–613. <https://doi.org/10.1016/j.memsci.2016.10.006>
- Lv J, Gong Z, He Z et al (2017) 3D printing of a mechanically durable superhydrophobic porous membrane for oil–water separation. *J Mater Chem A* 5:12435–12444. <https://doi.org/10.1039/C7TA02202F>
- Majouli A, Younssi SA, Tahiri S et al (2011) Characterization of flat membrane support elaborated from local Moroccan Perlite. *Desalination* 277:61–66. <https://doi.org/10.1016/j.desal.2011.04.003>
- Malik A, Kandasubramanian B (2018) Flexible polymeric substrates for electronic applications. *Polym Rev* 58:630–667. <https://doi.org/10.1080/15583724.2018.1473424>
- Mandal B (2002) Arsenic round the world: a review. *Talanta* 58:201–235. [https://doi.org/10.1016/S0039-9140\(02\)00268-0](https://doi.org/10.1016/S0039-9140(02)00268-0)
- Mazinani S, Al-Shimmery A, Chew YMJ, Mattia D (2019) 3D printed fouling-resistant composite membranes. *ACS Appl Mater Interfaces* 11:26373–26383. <https://doi.org/10.1021/acsami.9b07764>
- Mazumder S, Cole JV (2003) Rigorous 3-D mathematical modeling of PEM fuel cells. *J Electrochem Soc* 150:A1510. <https://doi.org/10.1149/1.1615609>
- Melenka GW, Cheung BKO, Schofield JS, Dawson MR, Carey JP (2016) Evaluation and prediction of the tensile properties of continuous fiber-reinforced 3D printed structures. *Compos Struct* 153:866–875. <https://doi.org/10.1016/j.compstruct.2016.07.018>
- Mishra N, Kandasubramanian B (2018) Biomimetic design of artificial materials inspired by iridescent nacre structure and its growth mechanism. *Polym-Plast Technol Eng* 57:1592–1606. <https://doi.org/10.1080/03602559.2017.1326139>
- Mohanraj G, Mao C, Armine A et al (2018) Ink-jet printing-assisted modification on polyethersulfone membranes using a UV-reactive antimicrobial peptide for fouling-resistant surfaces. *ACS Omega* 3:8752–8759. <https://doi.org/10.1021/acsomega.8b00916>
- Mousavi S, Deuber F, Petrozzi S et al (2018) Efficient dye adsorption by highly porous nanofiber aerogels. *Colloids Surfaces A Physicochem Eng Asp* 547:117–125. <https://doi.org/10.1016/j.colsurfa.2018.03.052>
- Ngo TD, Kashani A, Imbalzano G et al (2018) Additive manufacturing (3D printing): a review of materials, methods, applications and challenges. *Compos Part B Eng* 143:172–196. <https://doi.org/10.1016/j.compositesb.2018.02.012>
- Oliveira H (2012) Chromium as an environmental pollutant: insights on induced plant toxicity. *Aust J Bot* 2012:1–8. <https://doi.org/10.1155/2012/375843>
- Patrick L (2002) Mercury toxicity and antioxidants: Part 1: role of glutathione and alpha-lipoic acid in the treatment of mercury toxicity. *Altern Med Rev* 7:456–471
- Prasad A, Kandasubramanian B (2019) Fused deposition processing polycaprolactone of composites for biomedical applications. *Polym Technol Mater* 58:1365–1398. <https://doi.org/10.1080/25740881.2018.1563117>
- Rajhans A, Gore PM, Siddique SK, Kandasubramanian B (2019) Ion-imprinted nanofibers of PVDF/1-butyl-3-methylimidazolium tetrafluoroborate for dynamic recovery of europium (III) ions from mimicked effluent. *J Environ Chem Eng*. <https://doi.org/10.1016/j.jece.2019.103068>
- Rasal RM, Janorkar AV, Hirt DE (2010) Poly(lactic acid) modifications. *Prog Polym Sci* 35:338–356. <https://doi.org/10.1016/j.progpolymsci.2009.12.003>
- Rastogi P, Kandasubramanian B (2019a) Breakthrough in the printing tactics for stimuli-responsive materials: 4D printing. *Chem Eng J* 366:264–304. <https://doi.org/10.1016/j.cej.2019.02.085>
- Rastogi P, Kandasubramanian B (2019b) Review of alginate-based hydrogel bioprinting for application in tissue engineering. *Biofabrication* 11:042001. <https://doi.org/10.1088/1758-5090/ab331e>
- Rastogi S, Kandasubramanian B (2019c) Progressive trends in heavy metal ions and dyes adsorption using silk fibroin composites. *Environ Sci Pollut Res*. <https://doi.org/10.1007/s11356-019-07280-7>
- Rastogi P, Njuguna J, Kandasubramanian B (2019) Exploration of elastomeric and polymeric liquid crystals with photothermal actuation: a review. *Eur Polym J* 121:109287. <https://doi.org/10.1016/j.eurpolymj.2019.109287>
- Saini S, Kandasubramanian B (2018) Engineered smart textiles and Janus microparticles for diverse functional industrial applications. *Polym-Plast Technol Eng*:1–17. <https://doi.org/10.1080/03602559.2018.1466177>
- Sharma S, Balasubramanian K, Arora R (2016) Adsorption of arsenic (V) ions onto cellulosic-ferric oxide system: kinetics and isotherm studies. *Desalin Water Treat* 57:9420–9436. <https://doi.org/10.1080/19443994.2015.1042066>
- Shirazi SFS, Gharehkhani S, Mehrali M et al (2015) A review on powder-based additive manufacturing for tissue engineering: selective laser sintering and inkjet 3D printing. *Sci Technol Adv Mater* 16:033502. <https://doi.org/10.1088/1468-6996/16/3/033502>
- Shukla AK, Alam J, Alhoshan M et al (2018) Removal of heavy metal ions using a carboxylated graphene oxide-incorporated polyphenylsulfone nanofiltration membrane. *Environ Sci Water Res Technol* 4:438–448. <https://doi.org/10.1039/C7EW00506G>
- Shukla AK, Alam J, Ansari MA et al (2019) Selective ion removal and antibacterial activity of silver-doped multi-walled carbon nanotube/polyphenylsulfone nanocomposite membranes. *Mater Chem Phys* 233:102–112. <https://doi.org/10.1016/j.matchemphys.2019.05.054>
- Singh N, Kumar D, Sahu AP (2007) Arsenic in the environment: effects on human health and possible prevention. *J Environ Biol* 28:359–365
- Singh R, Gautam N, Mishra A, Gupta R (2011) Heavy metals and living systems: an overview. *Indian J Pharm* 43:246. <https://doi.org/10.4103/0253-7613.81505>
- Tan C, Zhou K, Ma W et al (2018) Selective laser melting of high-performance pure tungsten: parameter design, densification behavior and mechanical properties. *Sci Technol Adv Mater* 19:370–380. <https://doi.org/10.1080/14686996.2018.1455154>
- Tatem HE, Cox BA, Anderson JW (1978) The toxicity of oils and petroleum hydrocarbons to estuarine crustaceans. *Estuar Coast Mar Sci* 6:365–373. [https://doi.org/10.1016/0302-3524\(78\)90128-7](https://doi.org/10.1016/0302-3524(78)90128-7)
- Tijing LD, Dizon JRC, Ibrahim I et al (2020) 3D printing for membrane separation, desalination and water treatment. *Appl Mater Today* 18:100486. <https://doi.org/10.1016/j.apmt.2019.100486>

- Verma V, Balasubramanian K (2014) Experimental and theoretical investigations of Lantana camara oil diffusion from polyacrylonitrile membrane for pulsatile drug delivery system. *Mater Sci Eng C* 41: 292–300. <https://doi.org/10.1016/j.msec.2014.04.061>
- Vrouwenvelder JS, Graf von der Schulenburg DA, Kruithof JC et al (2009) Biofouling of spiral-wound nanofiltration and reverse osmosis membranes: a feed spacer problem. *Water Res* 43:583–594. <https://doi.org/10.1016/j.watres.2008.11.019>
- Withell A, Diegel O, Grupp I et al (2011) Porous ceramic filters through 3D printing. In: *Innovative developments in virtual and physical prototyping*. CRC Press, pp 313–318
- Wong KV, Hernandez A (2012) A review of additive manufacturing. *ISRN Mech Eng* 2012:1–10. <https://doi.org/10.5402/2012/208760>
- Xing R, Huang R, Qi W et al (2018) Three-dimensionally printed bioinspired superhydrophobic PLA membrane for oil-water separation. *AICHE J* 64:3700–3708. <https://doi.org/10.1002/aic.16347>
- Yadav R, Naebe M, Wang X, Kandasubramanian B (2017) Review on 3D Prototyping of Damage Tolerant Interdigitating Brick Arrays of Nacre. *Ind Eng Chem Res*
- Yadav R, Goud R, Dutta A et al (2018) Biomimicking of hierarchal molluscan shell structure via layer by layer 3D printing. *Ind Eng Chem Res* 57:10832–10840. <https://doi.org/10.1021/acs.iecr.8b01738>
- Yap CY, Chua CK, Dong ZL et al (2015) Review of selective laser melting: Materials and applications. *Appl Phys Rev* 2:041101. <https://doi.org/10.1063/1.4935926>
- Yap CY, Chua CK, Dong ZL (2016) An effective analytical model of selective laser melting. *Virtual Phys Prototyp* 11:21–26. <https://doi.org/10.1080/17452759.2015.1133217>
- Yap YL, Wang C, Sing SL et al (2017) Material jetting additive manufacturing: an experimental study using designed metrological benchmarks. *Precis Eng* 50:275–285. <https://doi.org/10.1016/j.precisioneng.2017.05.015>
- Yuan S, Wang J, Wang X et al (2015) Poly(arylene sulfide sulfone) hybrid ultrafiltration membrane with TiO₂-g-PAA nanoparticles: preparation and antifouling performance. *Polym Eng Sci* 55:2829–2837. <https://doi.org/10.1002/pen.24174>
- Yuan S, Strobbe D, Kruth J-P et al (2017a) Production of polyamide-12 membranes for microfiltration through selective laser sintering. *J Membr Sci* 525:157–162. <https://doi.org/10.1016/j.memsci.2016.10.041>
- Yuan S, Strobbe D, Kruth J-P et al (2017b) Super-hydrophobic 3D printed polysulfone membranes with a switchable wettability by self-assembled candle soot for efficient gravity-driven oil/water separation. *J Mater Chem A* 5:25401–25409. <https://doi.org/10.1039/C7TA08836A>
- Yuan S, Zhu J, Li Y et al (2019) Structure architecture of micro/nanoscale ZIF-L on a 3D printed membrane for a superhydrophobic and underwater superoleophobic surface. *J Mater Chem A* 7:2723–2729. <https://doi.org/10.1039/C8TA10249J>
- Zhakeyev A, Wang P, Zhang L et al (2017) Additive manufacturing: unlocking the evolution of energy materials. *Adv Sci* 4:1700187. <https://doi.org/10.1002/advs.201700187>

Publisher's note Springer Nature remains neutral with regard to jurisdictional claims in published maps and institutional affiliations.